Available online at www.sciencedirect.com
ScienceDirect
International Journal of Pharmaceutics 336 (2007) 248–256
INTERNATIONAL JOURNAL OF PHARMACEUTICS
www.elsevier.com/locate/ijpharm

Structural and thermal characterization of glyceryl behenate by X-ray diffraction coupled to differential calorimetry and infrared spectroscopy

J.B. Brubach [a,*], V. Jannin [b], B. Mahler [b], C. Bourgaux [d], P. Lessieur [c], P. Roy [a], M. Ollivon [d]

[a] *Synchrotron SOLEIL, Saint Aubin, 91192 Gif sur Yvette Cedex, France*
[b] *Gattefossé S.A.S., BP 603 69804, Saint-Priest Cedex, France*
[c] *UFR STMP, Université Nancy I, Domaine Scientifique Victor Grignard, BP 239, 54506 Vandoeuvre Cedex, France*
[d] *Laboratoire de Physicochimie des Systèmes Polyphasés, UMR 8612, Faculté de Pharmacie, 92296 Chatenay Malabry, France*

Received 5 May 2006; accepted 28 November 2006
Available online 2 December 2006

Abstract

Physical and thermal properties of glyceryl behenate (Compritol® 888 ATO) used as sustained-release matrix in pharmaceutical applications are studied by coupled time-resolved synchrotron X-ray diffraction and Differential Scanning Calorimetry combined with Infrared Spectroscopy. With these techniques, all polymorphs formed in glyceryl behenate, analyzed as received and after various thermal treatments from quenching to slow crystallization, are characterized. By using different well-controlled mixtures of mono-, di- and tribehenate, we identify each lamellar phase observed in the glyceryl behenate. Finally the influence of the crystallization rate on the formation of preferential conformations was also analyzed in order to bring insights into the polymorphism of glyceryl behenate. By changing the crystallization rate of the sample, it was shown that one can favor the formation of preferential polymorphs in the sample. In particular the crystallization at 10 °C/min seems to be well adapted for producing a single lamellar phase with a period of 60.9 Å while a crystallization rate of 0.4 °C/min produces three different lamellar phases.

Keywords: Excipient; Solid dosage forms; Lipids; Glyceryl behenate; Compritol® 888 ATO; X-ray diffraction; Differential scanning calorimetry

1. Introduction

Glycerides are a family of molecules used in the field of pharmaceutics as excipient mainly for solid dosage forms. Among them, Compritol® 888 ATO (glyceryl behenate, an atomized mixture of mono-, di- and tribehenate of glycerol) was first introduced on the pharmaceutical market as a solid-phase lubricant for tablet formulations (Jannin et al., 2003; N'Diaye et al., 2003). That excipient consists of a mixture of mono-, di- and tribehenate of glycerol (18%, 52% and 28% in weight, respectively) and presents a drop point ranging from 69 °C to 74 °C and a hydrophilic–lipophilic balance value of 2 (HLB is used as a measure of the polarity of the surface-active molecule). More recently, this mixture of glycerides has been designed to provide sustained release of drugs. Such release would not be obtained from more defined compound like pure di- or triglyceride. Hence, over the past decade, glyceryl behenate has been used for controlled-release applications by direct compression and more recently by: hot-melt coating (Barthélémy et al., 1999; Faham et al., 2000a,b), melt granulation or pelletization (Hamdani et al., 2002; Zhang and Schwartz, 2003) or the formation of solid–lipid nanoparticles (Freitas and Muller, 1999). This glyceride mixture is known to exhibit a complex polymorphism depending on many parameters such as crystallization rate or temperature of storage (Hamdani et al., 2003). As drug release depends on the stability of the crystalline structures formed, it is of prime importance to characterize any possible structural evolution of the excipient. Therefore, a description of the various structures formed as a function of time and temperature variations, is necessary both for the pharmaceutical science as it is linked to drug and excipient polymorphism and for a more general understanding of the thermal and structural behaviors of the glyceride mixtures (Small, 1986; Gunstone and Padley, 1997) which is also widely used in food and cosmetics. It is worth to remember that glycerides are naturally abundant molecules used for energy storage as well as building molecules in living systems. The mono-, di-, triglyceride mixture naturally results of lipase action and is of biological importance. Therefore, the

* Corresponding author. Tel.: +33 1 69 35 96 83; fax: +33 1 69 35 94 56.
E-mail address: jean-blaise.brubach@synchrotron-soleil.fr (J.B. Brubach).

0378-5173/$ – see front matter © 2006 Elsevier B.V. All rights reserved.
doi:10.1016/j.ijpharm.2006.11.057

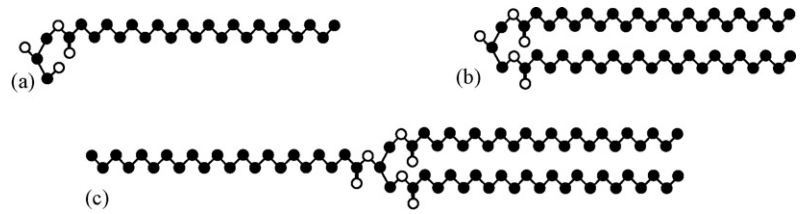

Fig. 1. Monobehenate (a), dibehenate (b) and tribehenate (c) of glycerol, the carbon and oxygen atoms are represented by black and white dots, respectively. For clarity the hydrogen atoms are not represented.

solid mixtures obtained with the long chain fatty acid are especially interesting candidates for controlled release of drugs. The amount of monoglycerides which are lyotropic molecules should be adjusted in these Generally Recognized As Safe (GRAS) mixtures to obtain the release expected.

Crystallization of glycerides has been the subject of an extensive literature exploiting the description of a variety of experimental tools (Pascher et al., 1981, 1992; Pascher, 1996; Goto et al., 1995; Di and Small, 1993). Such abundance of sources is related with the wide range of glycerides made from saturated or unsaturated acids, short or long chain acids, even or odd carbon numbered, mixed acid chains or mono acid chains, etc.

Lipid polymorphism is due to the numerous lateral packing possible of fatty acid chains specifically designated as sub α, α, β′ and β (Jackson and Lutton, 1950; Larsson, 1966; Chapman, 1962), each of them corresponding to a particular lateral organization of the hydrocarbon chains. In short: the most stable phase is the β variety for pure monoacid saturated triglyceride (TAGs), and the β′ phase for a mixture of fatty acids with long chains (De Jong and Van Soest, 1978), whereas the most stable phase for 1,2-diacyl-glycerol is β′ while the β variety is observed for 1,3-diacyl-glycerol (Kodali et al., 1990). A longitudinal stacking of the molecules in layers results of lateral packing. The stacking of lipid layers ranges from 1 to 6 chain layers with bilayers or trilayers, noted 2L or 3L, respectively, being the most frequently observed stacking. The crystalline phase is noted 2Lα for alpha bilayers lateral packing and 3Lβ for beta trilayers lateral packing. As a consequence of the diversity of possible structures formed, glycerides mixtures may exhibit a complex polymorphic behavior and the different structures developed by samples as a function of temperature or time are still unknown.

In this study, the structure and the polymorphic evolutions of glycerides mixtures, widely employed in controlled release formulations have been characterized by use of coupled X-Ray Diffraction and Differential Scanning Calorimetry. X-ray diffraction allows the study of the structure corresponding to both short reticular distances between hydrocarbon chains (lateral packing is observed in WAXS region) and long spacing (longitudinal stacking is observed in SAXS domain). Using temperature and enthalpy of transition measurements, DSC highlights energetic phenomena occurring during the heating or the cooling of the sample. By coupling these two techniques, we can link structural changes to phase transitions (Brubach et al., 2004). In addition, Infrared Spectroscopy has been used to determine chain positioning and conformation of glycerides at the molecular level.

The aim of this study is to evidence all possible polymorphs of Compritol® 888 ATO existing at room temperature for various rates of crystallization using simultaneous recordings of DSC coupled with SAXS and WAXS as a function of temperature from the same sample. The formation of these polymorphic forms will then be related to specific composition of Compritol® 888 ATO.

2. Materials and methods

Compritol® 888 was supplied by Gattefossé S.A.S, Saint Priest, (France) as an atomized (ATO) powder. Compritol® 888 ATO is synthesized by esterification of glycerol with behenic acid (C_{22} fatty acid) and therefore consists of a mix of monobehenate (Fig. 1a), dibehenate (Fig. 1b) and tribehenate (Fig. 1c) of glycerol, the diester fraction being predominant. Samples of monobehenate, dibehenate and tribehenate were also provided by Gattefossé S.A.S, Saint Priest, France (see Table 1).

X-ray diffraction measurements were performed at the D22 beam line of the synchrotron storage ring LURE-DCI, University of Paris Sud, Orsay, France. The D22 beam line allows high quality recording with low noise. Moreover SAXS, WAXS and DSC measurement data are collected simultaneously for sake of phase accuracy. The position sensitive linear detectors of SAXS and WAXS were calibrated, respectively, with silver behenate and tristearin (SSS) (Keller et al., 1998). All figures are presented

Table 1
Composition in monobehenate, dibehenate and tribehenate of each sample

	Monobehenate (%)	Dibehenate (%)	Tribehenate (%)
Compritol® 888 ATO	18	52	28
Dibehenate rich (Dibrich)	10	79	11
Tribehenate rich (Tribrich)	12.6	47.1	39.9
Monobehenate rich (Monobrich)	88	11	0.3
Tribehenate	0	0	100

as functions of the scattering vector, q (Å^{-1}) = ($2\pi/d$ (Å)) and the sample temperature (°C).

Microcalix version 2.0 has been used for DSC measurements (Keller et al., 1998). Briefly, samples were prepared by introduction of a fixed amount (20–25 mg) of sample powder in a calibrated Lindeman glass capillary (GLAS-Muller, Berlin). DSC temperature was standardized using lauric acid second melting as previously described (Hernquist and Larsson, 1982). X-ray data have been analyzed using a subroutine developed under Igor 4.1 by F. Artzner.

The IR transmission spectra of the sample were recorded using a Bomem DA8 Fourier transform spectrometer, under vacuum, at the SIRLOIN beam line (Roy et al., 1995, 1998; Mathis et al., 1998) at super-Aco synchrotron ring, LURE, University of Paris Sud, Orsay, France. The Mid-infrared region (500–9000 cm^{-1}) was investigated thanks to a globar source, in combination with a KBr beam splitter and a MCT wide range detector. Spectra were recorded with a resolution of 2 cm^{-1} with 200 scans per spectrum and no mathematical correction (e.g., smoothing) was performed. Transmission measurements of both reference and sample were recorded using a variable path cell equipped with two 0.5 mm thick diamond windows. The sample was melted at 90 °C and then crystallized at 0.4 °C/min to 10 °C. Infrared spectra were recorded every 10 min from 77 °C to 22 °C at 0.4 °C/min.

3. Results and discussion

3.1. Structural and thermal studies of glyceryl behenate

Glyceryl behenate was first analyzed during heating at 0.4 °C/min without any special thermal treatment (as received). Fig. 2 represents the evolution of the position and the intensity (size of the symbols) of each diffraction peak observed in SAXS together with DSC recording (full line) in the temperature domain 10 °C ≤ T ≤ 90 °C. The useful domain of the scattering vector q (Å^{-1}) ranges from 0.085 Å^{-1} to 0.42 Å^{-1}.

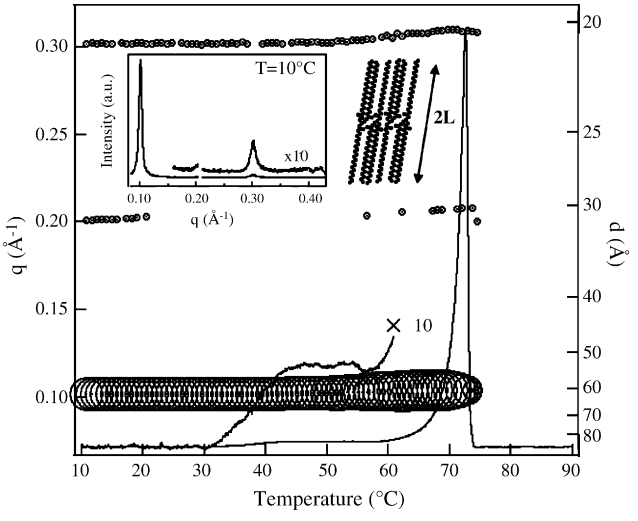

Fig. 2. DSC recording and SAXS evolution during the first heating of a sample of glyceryl behenate mixture analyzed as-received at 0.4 °C/min. Circles indicate the position (in q (Å^{-1}) and d (Å)) and the intensity (size of the symbol) of each peak observed in SAXS. DSC recording (and DSC signal ×10) recorded simultaneously is superimposed to help the interpretation of SAXS data. *Inset*: SAXS pattern at T = 10 °C.

The DSC recording observed on slow heating of stabilized Compritol® sample shows a main sharp melting endotherm at about 70 °C. This sharp peak is preceded by a broad endotherm spreading from about 35 to about 60 °C.

At T = 10 °C (inset of Fig. 1), a single lamellar phase is observed with Bragg reflections in the positional ratio 1:2:3 corresponding, respectively, to q (Å^{-1}) values at 0.101 Å^{-1}, 0.201 Å^{-1} and 0.302 Å^{-1} (respectively, 61.8 Å, 31.3 Å and 20.8 Å). The relative intensity of each peak, with the first order more intense than the third order, itself more intense than the second order, corresponds to a lamellar phase of 61.8 Å under a 2L conformation of molecules (see drawing in the inset of Fig. 2).

No change in position and width is observed until the temperature reaches 39.5 °C from where a regular shift toward higher q (Å^{-1}) values is observed, corresponding to a decrease of the lamellar long distance from 61.8 Å to 60.4 Å for the main peak. This is followed from T_{onset} = 49 °C by a regular increase of this intensity of the line (around +28%) which reaches a maximum at T = 67 °C. Finally at T_{onset} = 71 °C, the complete melting of the sample is observed.

Simultaneously, for the WAXS domain (Fig. 3a and b), at T = 10 °C, the two strong peaks corresponding to short spacing at 1.5 Å^{-1} and 1.65 Å^{-1} (respectively, 3.8 Å and 4.2 Å) indicate the presence of a sub α phase (Jackson and Lutton, 1950; Chapman, 1962; Kodali et al., 1990) in the lateral packing of chains. This less ordered phase develops a pseudohexagonal lattice which is similar to the packing of the orthorhombic perpendicular subcell of the β′ phase of TAGs (Jackson and Lutton, 1950; Chapman, 1962). As the temperature is raised, a regular shift toward the low q values of the line at 1.65 Å^{-1} can be noticed. This shift starts at about 35 °C and develops up to about 60 °C (Fig. 3, top). It corresponds to the very broad low-enthalpy transition observed on the DSC curve. At T > 55–60 °C, only a single strong short spacing is observed at 1.50 Å^{-1} (4.18 Å). This strong wide angle diffraction line indicates the formation of a hexagonal packing also noted α. Therefore, these structural changes are interpreted as a sub α to α transition similar to that observed in alcanes (Doucet et al., 1981; Small, 1986). This progressive transition leads to the small endothermic event spreading in the range 35–60 °C described above. It is worth to note that this transition precedes the decrease of the lamellar period from 61.8 Å to 60.4 Å and the increase of 28% of the peak intensity.

Finally, at T_{onset} = 71 °C, the melting of the sample corresponds to the complete disappearance of the peak at 1.50 Å^{-1} and the appearance of a broad short spacing centered at 4.6 Å characteristic of the liquid phase.

As established previously, the glyceryl behenate mixture analyzed as received develops a lamellar phase of 61.8 Å with a 2L conformation and a pseudo-hexagonal subcell noted sub α at ambient temperature. This conformation can be related to the composition of Compritol® 888 ATO which includes

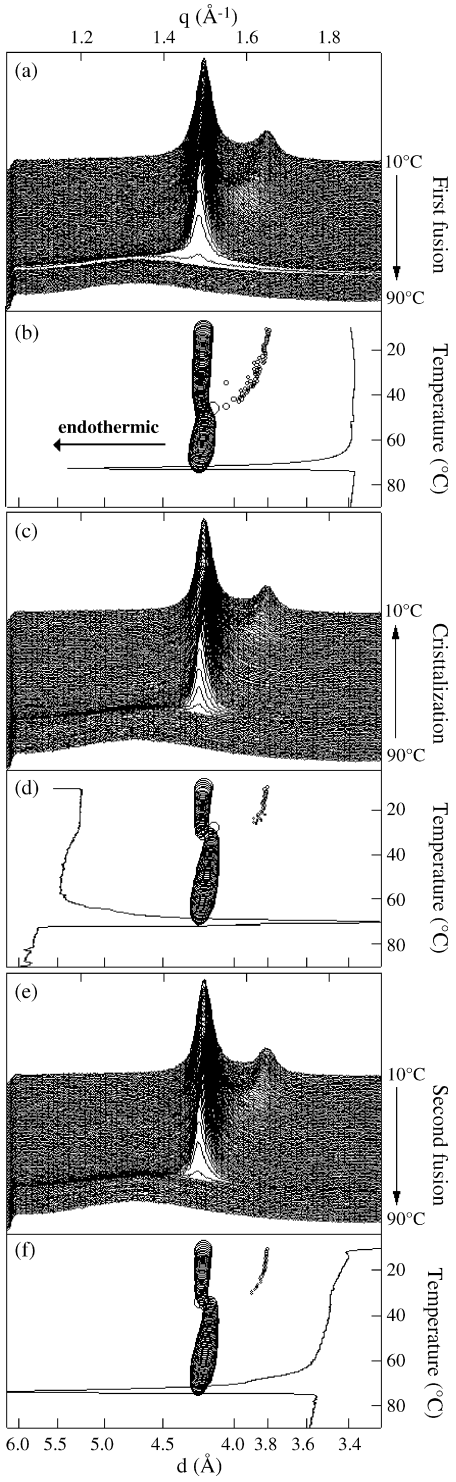

Fig. 3. Evolution of WAXS patterns with the temperature shown together with DSC recording for (a) the first fusion (c) the crystallization (e) the second fusion of an untreated sample of glyceryl behenate at 0.4 °C/min. (b, d, f) Position and intensity (size of the symbol) of each peak observed in WAXS for the same temperature events.

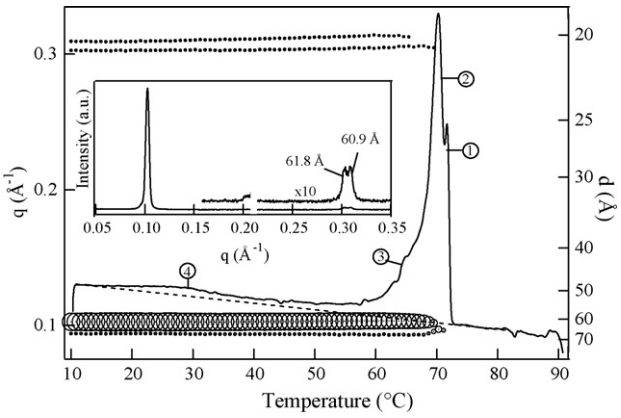

Fig. 4. Evolution of position and intensity (size of the symbol) of each line observed in SAXS during the crystallization of the sample at 0.4 °C/min. Inset SAXS pattern at $T = 10$ °C. DSC curve recorded simultaneously and its different steps noted 1–4 are shown for comparison with SAXS evolution.

approximately 52% of dibehenate. Such conformation has already been observed in 1,2-diglycerides with long fatty acid chains such as C_{22} and C_{24} by Kodali et al. (1990) and in monoglycerides as 1-monostearin and 1-monopalmitin by Lutton and Jackson (1948). Upon melting, the long spacing of this lamellar phase is found to decrease in size from 61.8 Å to 60.4 Å and to adopt a hexagonal packing noted α. Both conformations are the most stable phases and therefore the most ordered ones. The apparently reversible transition observed between sub α and α is similar to that of alcanes rather than that observed for glycerides (Doucet et al., 1981; Small, 1986) since no signature of a β′ phase characterized by three strong short distance peaks at 4.3 Å, 4.15 Å and 3.75 Å is observed (Kodali et al., 1990). Moreover, no particular signatures of the tribehenate, which represents approximately 28% (mass ratio) of the sample, are observed by X-ray diffraction or DSC.

Fig. 4 presents the crystallization of Compritol® 888 ATO observed on cooling at 0.4 °C/min after having been maintained 10 min at 90 °C. Four thermal events noted 1–4 occur before the complete crystallization of the sample and can be attributed to the formation of specific structures. At $T_{onset} = 72.5$ °C, a first single lamellar phase of 65.1 Å is formed (Step 1 on DSC recording). Then, at $T_{onset} = 71.5$ °C, the peak diffraction splits in two peaks corresponding to two lamellar phases with 61.0 Å (major one) and 66.8 Å long spacing (Step 2).

At $T_{onset} = 68.5$ °C, a third lamellar phase with a long period of 59.9 Å can be observed (Step 3). The long period of each lamellar phase is deduced from the position of its third order due to the small difference of size between the different lamellar phases (inset of Fig. 3).

From $T = 68.5$ °C to the last thermal events at $T = 38.5$ °C, the two long distances of these lamellar phases gradually increases: the first lamellar phase passing from 61.0 Å to 61.8 Å at $T = 38.5$ °C, the second one passing from 59.9 Å to 60.9 Å at approximately $T = 27$ °C (Step 4). Finally at $T = 10$ °C, three lamellar phases of 66.8 Å, 61.8 Å and 60.9 Å are observed in the Compritol® 888 ATO sample.

For the WAXS domain, this last thermal event at $T = 38.5$ °C corresponds to the transition from one single short spacing at 1.5 $Å^{-1}$ (4.2 Å) to two strong short spacings at 1.5 $Å^{-1}$ and 1.65 $Å^{-1}$ (respectively, 3.8 Å and 4.2 Å) corresponding to a α → sub α transition. We can then attribute this transition to

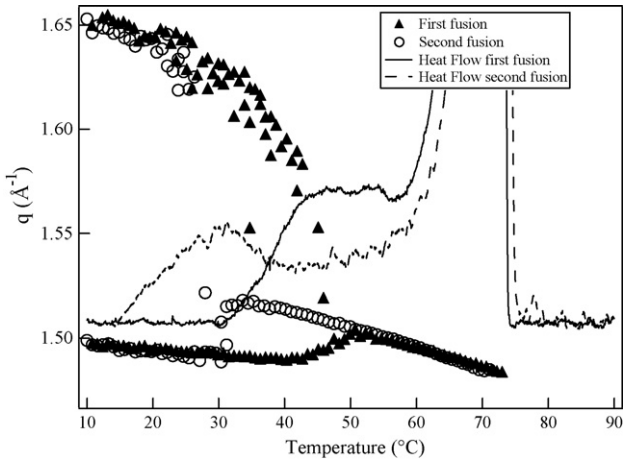

Fig. 5. Evolution of the peak positions in WAXS and DSC curves obtained simultaneously during the first and the second fusion of glyceryl behenate mixture.

the stabilization of the long spacing of the two lamellar phases at 60.9 Å and 61.8 Å.

The sequence of transitions observed upon cooling is reversible during the second heating of the sample, except for the lamellar phase at 65.1 Å which is not observed before the first complete melt of the sample, whereas this long distance has been observed to be the first to crystallize.

Moreover, for the WAXS domain, the temperature of the sub $\alpha \rightarrow \alpha$ transition is different for the first and the second fusion of the sample (Fig. 5). A large gap is observed between these two transitions: occurring at $T = 49\,^{\circ}C$ for the first fusion and $T = 30\,^{\circ}C$ for the second fusion. We can link this observation to the formation of a second variety sub α noted sub α_2 presenting a lower temperature of transition to a α variety than the variety sub α_1 observed during the first fusion. This new "sub α_2" can also be associated to the new lamellar phase of 60.9 Å observed during the crystallization of glyceryl behenate mixture. Therefore, two lamellar phases, 61.8 Å and 60.9 Å, presenting two different substructures, respectively, sub α_1 and sub α_2 exist after crystallization. The third lamellar phase of 66.8 Å, minor in proportion with respect to the relative intensity of the diffraction peak, may develop an hexagonal subcell or α variety, as its long distance diffraction peaks presents no modification in position width and intensity.

Fig. 6 presents the thermal and structural evolution of the glyceryl behenate mixture during the first and the second fusion of the same sample at a heating rate of 2 °C/min.

During the second fusion of the sample, because of the higher rate of heating employed, the two thermal events corresponding to the transition from the sub α_1 and the sub α_2 varieties to, respectively, the α_1 and α_2 varieties are clearly observable. In both cases, the α variety corresponding to a hexagonal subcell is the most stable variety observed at high temperature. After crystallization three lamellar phases presenting three different long spacings are observed.

Compritol® 888 ATO is synthesized by esterification of glycerol with behenic acid (C_{22} fatty acid) and therefore consists of a mix of mono-, di- and tribehenate, the diester fraction being

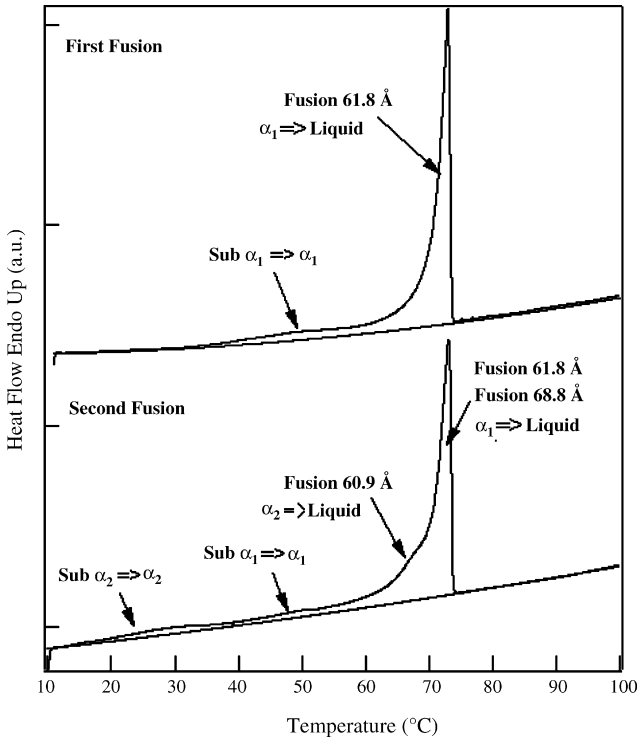

Fig. 6. DSC curves and structural changes observed in SAXS and WAXS during the first and the second fusion of crystals of glyceryl behenate mixture.

predominant. Such composition may explain the complex polymorphic behavior of the sample. Therefore we can assume that the crystallization behavior may reflect the competition between each species within glyceryl behenate mixture.

3.2. Infrared study

Infrared spectroscopy has been extensively used to characterize lipids (Yano et al., 1997; Chapman, 1965) and is a powerful tool for the investigation of the molecular conformation of glycerides as marked changes in the spectra occurs between one polymorphic form to another. In particular the vibrational bands of the CH_2 groups appear to be sensitive to the crystal structure of the glycerides.

Fig. 7 presents several vibrational bands of rocking, bending, wagging and twisting of the methylene group (–CH_2–) located in the region between 700 cm^{-1} and 1500 cm^{-1}, revealing the structural changes as the sample is cooled down. These changes can be related to those observed by X-ray diffraction (Figs. 3c–d and 4) for which the same crystallization rate of 0.4 °C/min was used.

The infrared spectra for $T < 71\,^{\circ}C$ is dominated by the –CH_2– crystalline structure. The single bands at 1467 cm^{-1} and 721 cm^{-1} are, respectively, characteristics of the CH_2 scissoring $\delta(CH_2)$ and the CH_2 rocking $r(CH_2)$. For the same temperature, definite evidence of crystallization of the sample is observed for the CH_2 wagging and twisting modes located in the 1150–1350 cm^{-1} region where a number of bands, proportional to the number of carbon atom in the chain, arise. These bands position and shape are usually assigned to the α

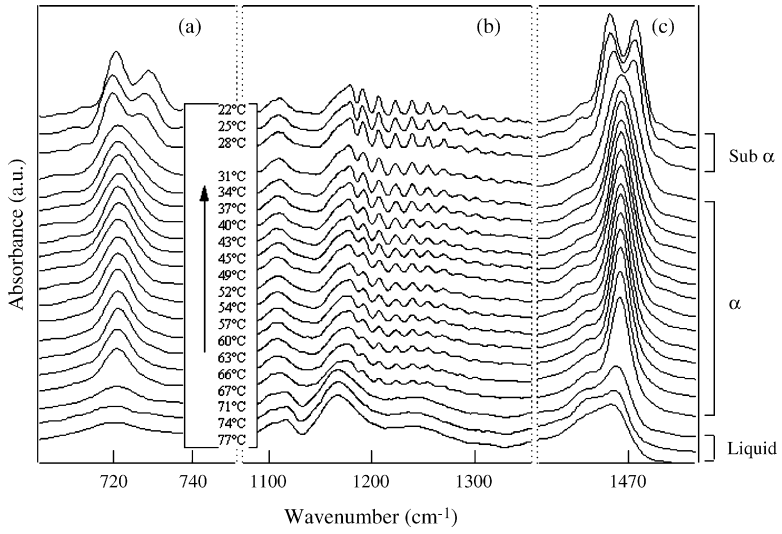

Fig. 7. Mid infrared spectra recorded during the crystallization at 0.4 °C/min between 77 °C and 22 °C of glyceryl behenate mixture. (a) CH_2 rocking r(CH_2), (b) wagging ω(CH_2) and twisting τ(CH_2), (c) CH_2 scissoring δ(CH_2).

subcell corresponding to the hexagonal conformation of the subcell (Chapman, 1965; Dohi et al., 2002).

The second series of changes is observed for $T < 31$ °C where the single bands due to the CH_2 scissoring $\delta(CH_2)$ and the CH_2 rocking $r(CH_2)$ split into a doublet at 720 cm^{-1} and 728 cm^1 for the rocking mode and at 1464 cm^{-1} and 1472 cm^{-1} for the scissoring mode. Notice that for the same temperature, X-ray diffraction, revealed the split of the 4.2 Å peak into two peaks at 3.8 Å and 4.2 Å. The changes in the IR band shape are commonly attributed to a change in the conformation of the methylene chain to a β′ variety or to a sub α variety as this last type of subcell presents a packing similar to the orthorhombic perpendicular subcell of the β′ variety. Moreover, for the wagging and twisting region, no change is observed in the position, intensity or shape. Previous studies on this IR region have shown important changes in band position and intensity during the transition to a β′ variety from a α variety (Yano et al., 1997; Yano and Sato, 1999; Chapman, 1965). Therefore the lack of modification of these bands supports a transition from a α variety to sub α variety. Consequently the sub α variety appears to be intermediate between the two varieties α and β′: the subcell structure along the short axis of the acyl chains is changed into an orthorhombic perpendicular subcell (like the β′ variety) and the long spacing indicates that there is no tilt change along the long axis and consequently no modification of the wagging and twisting bands in the infrared spectra (as in the α variety).

3.3. Structural study of various compositions of mono-, di- and tribehenate

In order to associate each lamellar phase observed previously to a particular compound of the Compritol® 888 ATO, several samples consisting of well-controlled mixtures of mono-, di- and tribehenate have been studied (Table 1).

All samples were studied by X-ray diffraction in the SAXS and WAXS domains. As it was not possible to distinguish the species from the first and the second order of SAXS patterns, only the third order reflexions and above were exploited. Fig. 8 represents the third order of each lamellar phase in SAXS pattern obtained at 10 °C for Compritol® 888 ATO and the three new samples. Simultaneously, a unique conformation in the WAXS domain corresponding to a pseudohexagonal subcell (not represented here) was observed for all samples.

By comparing the position of each diffraction peak, it appears that the two lamellar phases observed at 60.9 Å and 61.8 Å during the second fusion of Compritol® 888 ATO can be correlated, respectively, to the sample of tribehenate and Dibehenate rich (Dirich). It can therefore be deduced that the dibehenate within the Compritol® 888 ATO is responsible for the formation of a lamellar phase of 61.8 Å with a sub α_1 subcell at room temperature. And the tribehenate part of the Compritol® 888 ATO is responsible for the formation of a lamellar phase of 60.9 Å with a sub α_2 subcell at room temperature (see Fig. 5).

To verify whether the 60.9 Å lamellar phase observed corresponds to the tribehenate fraction, we changed the proportion

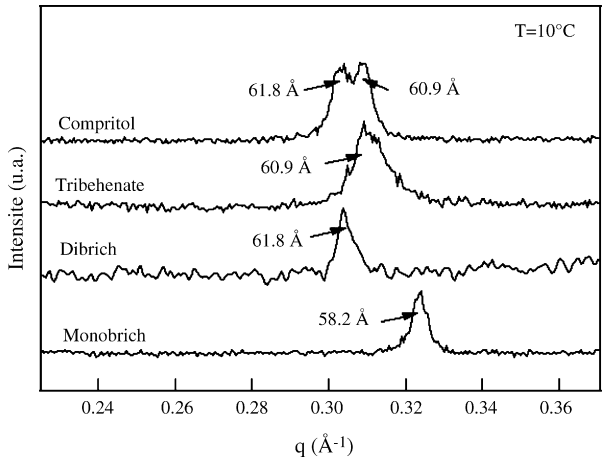

Fig. 8. SAXS recordings obtained at 10 °C for Compritol® 888 ATO, tribehenate, dibehenate rich and monobehenate rich samples after crystallization. For all these samples a sub α subcell was observed at 10 °C in the WAXS domain.

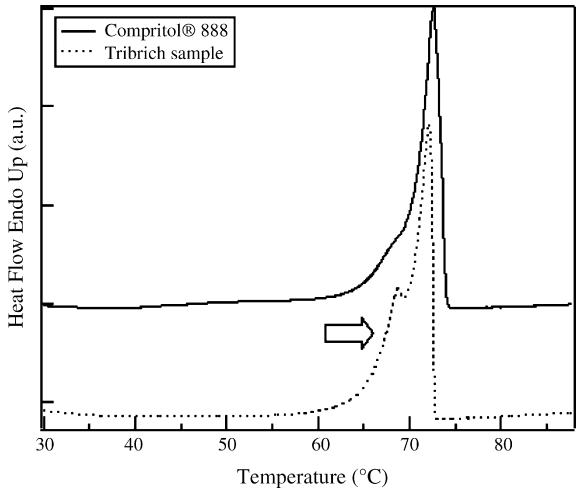

Fig. 9. Comparison of the DSC traces recorded between 0 °C and 100 °C at 1 °C/min for the untreated Compritol® 888 ATO containing (18%, 52% and 28%) and the tribehenate rich sample containing (12.6%, 47.1%, 39.9%) in mono-, di- and tribehenate.

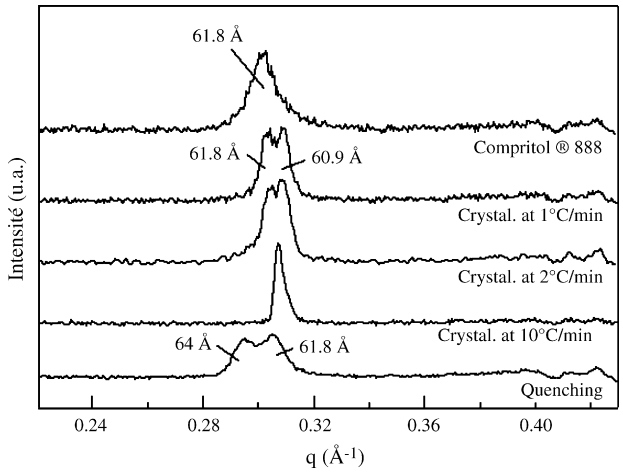

Fig. 10. SAXS patterns at $T = 10\,^{\circ}C$ of the third order of untreated Compritol® 888 ATO and for samples of Compritol® 888 ATO crystallized at cooling rates of 1 °C/min, 2 °C/min, 10 °C/min and quenched into liquid nitrogen.

in the sample and observed corresponding DSC changes in the thermal profile. Fig. 9 represents the DSC curves obtained from two samples made of 28% (untreated Compritol® 888 ATO) and 39.9% (Tribehenate rich) of tribehenate. Indeed as the concentration of tribehenate is increased in the sample, the thermal event located at $T_{onset} = 65.3\,^{\circ}C$ significantly increase. Therefore, the thermal event at $T_{onset} = 65.3\,^{\circ}C$ is clearly due to the fusion of tribehenate molecules organized in a 2L lamellar phase with a long period of 60.9 Å. In turn, the last thermal event at $T_{onset} = 69\,^{\circ}C$ can be associated to the fusion of the dibehenate fraction of the sample.

3.4. Influence of the crystallization rate on the structure

The influence of the crystallization rate on the formation of preferential conformations was analyzed in order to bring insights into the polymorphism of Compritol® 888 ATO. For this purpose, we compared the X-ray diffraction patterns recorded in SAXS and WAXS domain for three samples held 10 min at 90 °C and then crystallized at three different cooling rates. The first sample was quenched into liquid nitrogen, the second and the third one were cooled down to 10 °C at respective rates of 2 °C/min and 10 °C/min. For the rapid cooling rate, X-ray diffraction patterns were recorded at 10 °C. For the two progressive rates, X-ray diffraction patterns were also collected during sample cooling (one measurement per minute). Fig. 10 displays SAXS patterns obtained at $T = 10\,^{\circ}C$ for the untreated sample of Compritol® 888 ATO and after crystallization at different rates. For clarity, only the third order of the diffraction peak is presented as describe before.

It can be noticed that crystallizations at 2 °C/min and 1 °C/min lead to the formation of the same two lamellar phases of 61.8 Å and 60.9 Å but in slightly different proportions (Fig. 10).

The crystallization by quenching into liquid nitrogen produces two lamellar phases of 61.8 Å and 64 Å. In the crystallization at 1 °C/min, the 64 Å phase is the first to crystallize (Fig. 9). After subsequent cooling it leads to the formation of lamellar phases at 61.8 Å and 66.5 Å. Both lamellar phases of 61.8 Å and 64 Å display a sub α subcell (not shown) at wide angles.

In contrast, the crystallization at 10 °C/min leads to the formation of a single 60.9 Å lamellar phase. Consequently this rate of crystallization seems to be well adapted for producing a single lamellar phase. However, a peculiar behavior can be observed upon careful examination of the sample fast crystallization (Fig. 11). The crystallization firstly produces a lamellar phase under a α subcell at $T = 76\,^{\circ}C$ ($d = 59.5$ Å), then the cooling of the sample to 63 °C at 10 °C/min leads to the transition from the α to a β′ subcell characterized by three diffraction peaks at 4.45 Å, 4.2 Å and 3.94 Å. For this subcell, a new lamellar long period of 60.2 Å is observed. Surprisingly, this lamellar phase described as a more stable subcell (Small, 1986; Jackson and Lutton, 1950) transits at 42 °C to an apparently less stable subcell ($d = 60.9$ Å) noted sub α. No further change in the subcell or the long period of the lamellar phase of 60.9 Å is observed until the sample reaches 10 °C.

Table 2 summarizes the various conformations and phase transitions observed in Compritol® 888 ATO as a function of the crystallization rate (from quenching into liquid nitrogen to 1 °C/min). Each lamellar phase is attributed to a particular type of glycerides present in Compritol® 888 ATO.

The crystallization rate of the glyceryl behenate mixture appears to be the main factor that governs the adoption of a particular structure. For slow crystallization rates, each glyceride will crystallize separately and will produce a complex matrix containing several lamellar phases which could present several rates of drug release. Therefore such thermal treatment is not suitable for the production of pharmaceutical solid dosage form. Inversely a crystallization rate of 10 °C/min or more will favor the formation of a unique lamellar phase dominated by the triglycerides part of the sample together a pseudo-hexagonal subcell noted sub α imposed by the diglycerides (Kodali et al., 1990) and the monoglycerides (Lutton and Jackson, 1948). At the beginning of the crystallization the long and short range

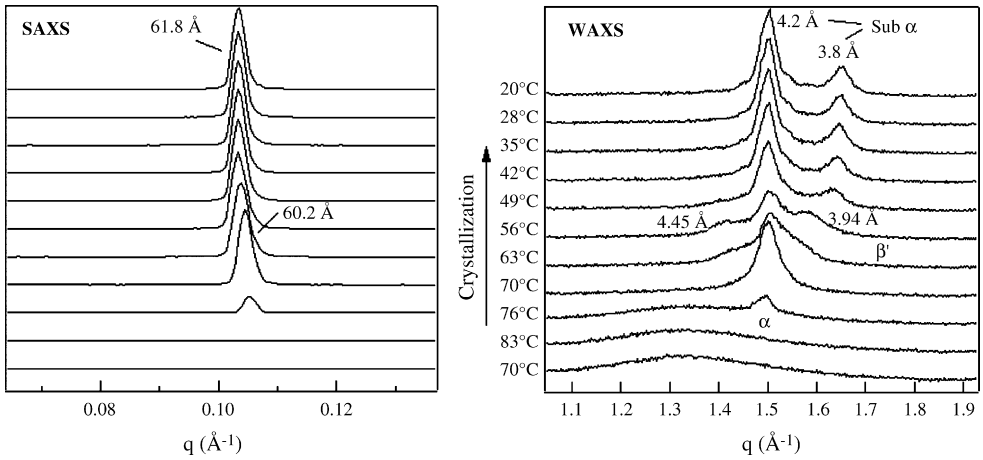

Fig. 11. SAXS and WAXS patterns obtained during the crystallization of Compritol® 888 ATO between 90 °C and 10 °C at 10 °C/min.

Table 2
Conformations and phase transitions observed in Compritol® 888 ATO as a function of the crystallization rate

Rate	Transition upon cooling	Room temperature
Compritol® 888 ATO as received (stabilized)		Sub α 2L 61.8 Å Dibehenate
Quenching		Sub α Sub α 2L + 2L 64 Å 61.8 Å ? Dibehenate
at 10°C/min	α (63°C) β' (42°C) 2L → 2L → 59.5 Å 60.2 Å	Sub α 2L 60.9 Å Tribehenate
at 1°C/min	α (71.5°C) α α α (38.5°C) 2L → 2L + 2L + 2L → 65.1 Å 59.9 Å 61.0 Å 66.8 Å Tribehenate Dibehenate ?	Sub α Sub α ? 2L + 2L + 2L 60.9 Å 61.8 Å 66.8 Å Tribehenate Dibehenate ?

conformation is given by the triglyceride part of the sample as evidenced by the lamellar phase of 60.9 Å observed with a α subcell and with a β′ subcell under 63 °C. Under 42 °C, the diglyceride part, predominant in proportion (52%), governs the crystallization of the sample and, the period of 60.9 Å is conserved for the lamellar long spacing with a sub α conformation.

4. Conclusion

The combination of X-ray diffraction at both small and wide angles with DSC and infrared spectroscopy at various temperature and phase has enabled us to characterize all the polymorphs displayed by Compritol® 888 ATO, taken as a typical glyceryl behenate mixture. The description of the polymorphism of this excipient is of paramount importance for pharmaceutical science since drug release control is closely linked to excipient structure. We have shown that the formation of the different phases is dominated by the thermal history (time and temperature) as well as by the sample composition.

By changing the crystallization rate of the sample, we have shown that we can favor the formation of preferential polymorphs in the sample. Namely, the crystallization at 10 °C/min seems to be well adapted for producing a single lamellar phase of a single 60.9 Å. For this rate, however, we have evidenced a specific behavior of the sample which present a complex structural evolution during the crystallization passing from a α variety to a β′ variety (at $T = 63$ °C) and finally to a sub α variety at 10 °C. The fast cooling of glyceryl behenate mixture leads to single metastable form which could be exploited for constant and well controlled drug release.

References

Barthélémy, P., Laforêt, J.P., Farah, N., Joachim, J., 1999. Compritol 888 ATO: an innovative hot-melt coating agent for prolonged-release drug formulations. Eur. J. Pharm. Biopharm. 47, 87–90.

Brubach, J.B., Ollivon, M., Jannin, V., Mahler, B., Bourgaux, C., Lesieur, P., Roy, P., 2004. Structural and thermal characterization of mono- and di-acyl polyoxyethylene glycol by infrared spectroscopy and X-ray diffraction coupled to differential Calorimetry. J. Phys. Chem. B 108, 17721–17729.

Chapman, D., 1965. The Structure of Lipids by Spectroscopic and X-ray Techniques. Methuen and Co. Ltd., London.

Chapman, D., 1962. Polymorphism of glycerides. Chem. Rev. 62, 433–456.

De Jong, S., Van Soest, T.C., 1978. Crystal structures and melting points of saturated triglycerides in the β-2 phase. Acta Crystallogr. B 34, 1570–1583.

Di, L., Small, D.M., 1993. Physical behavior of the mixed chain diacylglycerol, 1-stearoyl-2-oleyl-sn-glycerol: difficulties in chain packing produce marked polymorphism. J. Lipid Res. 34, 1611–1623.

Dohi, K., Kaneko, F., Kawaguchi, T., 2002. X-ray and vibrational spectroscopic study on polymorphism of trielaidin. J. Cryst. Growth 237–239, 2227–2232.

Doucet, J., Denicolo, I., Craievich, A., 1981. Evidence of a phase transition in the rotator phase of the odd-numbered paraffins $C_{23}H_{48}$ and $C_{25}H_{52}$. J. Chem. Phys. 75, 5125–5127.

Faham, A., Prinderre, P., Farah, N., Eichler, K.D., Kalantzis, G., Joachim, J., 2000a. Hot-melt coating technology. I: Influence of Compritol 888 ATO and granule size on theophylline release. Drug Dev. Ind. Pharm. 26, 167–176.

Faham, A., Prinderre, P., Piccerelle, P., Farah, N., Joachim, J., 2000b. Hot melt coating technology: Influence of Compritol 888 ato and granule size on chloroquine release. Pharma 55, 444–448.

Freitas, C., Muller, R.H., 1999. Correlation between long-term stability of Solid Lipid Nanoparticles (SLN) and crystallinity of the lipid phase. Eur. J. Pharm. Biopharm. 47, 125–132.

Goto, M., Honda, K., Di, L., Small, D.M., 1995. Crystal structure of a mixed chain diacylglycerol, 1-stearoyl-3-oleyl-glycerol. J. Lipid Res. 36, 2185–2190.

Gunstone, F.D., Padley, F.B., 1997. Lipid Technologies and Applications. Marcel Dekker Inc., New York.

Hamdani, J., Moës, A.J., Amighi, K., 2002. Development and evaluation of prolonged release pellets obtained by the melt pelletization process. Int. J. Pharm. 245, 167–177.

Hamdani, J., Moës, A.J., Amighi, K., 2003. Physical and thermal characterisation of Precirol® and Compritol® as lipophilic glycerides used for the preparation of controlled-release matrix pellets. Int. J. Pharm. 260, 47–57.

Hernquist, L., Larsson, K., 1982. Fette Seifen Anstrichm. 84, 349–354.

Jackson, F.L., Lutton, E.S., 1950. The polymorphism of certain behenyl mixed triglycerides. A new metastable crystalline form of triglycerides. J. Am. Chem. Soc. 72, 4519–4521.

Jannin, V., Bérard, V., N'Diaye, A., Andrès, C., Pourcelot, Y., 2003. Comparative study of the lubricant performance of Compritol® 888 ATO either used by blending or by hot melt coating. Int. J. Pharm. 262, 39–45.

Kodali, D.R., Fahey, D.A., Small, D.M., 1990. Structure and polymorphism of saturated monoacid 1,2-diacyl-sn-glycerols. Biochemistry 29, 10771–10779.

Keller, G., Lavigne, F., Forte, L., Andrieux, K., Dahim, M., Loisel, C., Ollivon, M., Bourgaux, C., Lesieur, P., 1998. J. Therm. Anal. Calorim. 51, 738–791.

Larsson, K., 1966. Classification of glyceride crystal forms. Acta Chem. Scand. 20, 55–2260.

Lutton, E.S., Jackson, F.L., 1948. The polymorphism of 1-monostearin and 1-monopalmitin. J. Am. Chem. Soc. 70, 2445–2449.

Mathis, Y.-L., Roy, P., Tremblay, B., Nucara, A., Lupi, S., Calvani, P., Gerschel, A., 1998. Magnetic field discontinuity as a new brighter source of infrared synchrotron radiation. Phys. Rev. Lett. 80, 1220–1223.

N'Diaye, A., Jannin, V., Bérard, V., Andrès, C., Pourcelot, Y., 2003. Comparative study of the lubricant performance of Compritol® HD5 ATO and Compritol® 888 ATO: effect of polyethylene glycol behenate on lubricant capacity. Int. J. Pharm. 254, 263–269.

Pascher, I., Sundull, S., Hauser, H., 1981. Glycerol conformation and molecular packing of membrane lipids: the crystal structure of 2,3-dilauroyl-D-glycerol. J. Mol. Biol. 153, 791–806.

Pascher, I., Lundmark, M., Nyholm, P.-G., Sundell, S., 1992. Crystal structures of membrane lipids. Biochim. Biophys. Acta 1113, 339–373.

Pascher, I., 1996. The different conformations of the glycerol region of crystalline acylglycerols. Curr. Opin. Struct. Biol. 6, 439–448.

Roy, P., Mathis, Y.-L., Lupi, S., Nucara, A., Tremblay, B., Gerschel, A., 1995. Synchrotron Radiat. News 5, 415.

Roy, P., Mathis, Y.-L., Paolone, A., Giura, P., Nucara, A., Lupi, S., Calvany, P., Gerschel, A., 1998. Nuovo Cimento. Soc. Ital. Fis. 20D, 415.

Small, D.M., 1986. The Physical Chemistry of Lipids, From Alkanes to Phospholipids. Handbook of Lipid Research, vol. 4. Plenum Press, New York/London, pp. 345–394.

Yano, J., Kaneko, F., Kobayashi, M., Sato, K., 1997. Structural analyses of triacylglycerol polymorphs with FT-IR techniques. 1: Assignments of CH_2 progression bands of saturated monoacid triacylglycerols. J. Phys. Chem. B 101, 8112–8119.

Yano, J., Sato, K., 1999. FT-IR studies on polymorphism of fats: molecular structures and interactions. Food Res. Int. 32, 249–259.

Zhang, Y.E., Schwartz, J.B., 2003. Melt granulation and heat treatment for wax matrix-controlled drug release. Drug Dev. Ind. Pharm. 29, 131–138.